LASERS

PACS numbers: 42.55.Px; 07.07.Hj; 42.62.-b
DOI: 10.1070/QE2002v032n04ABEH002187

Temperature regime of the laser screen of a cathode-ray tube

V.I.Kozlovsky, Kh.Kh.Kumykov, I.V.Malyshev, Yu.M.Popov

***Abstract*. The temperature regime of a laser cathode-ray tube are studied upon the electron-beam raster scanning. Three main factors determining the temperature of the active region of a laser are distinguished: the adiabatic heating by the electron beam during excitation of an individual pixel, heating caused by adjacent lines, and heating averaged during previous scans, which is determined by cooling of the laser screen. The numerical estimates of the temperature rise caused by these factors are presented. The influence of the temperature of the active region on the lasing power is discussed.**

Keywords: *laser screen, cathode-ray tube, temperature regime.*

1. Introduction

A laser cathode-ray tube (LCRT) provides the display of information, including TV images, with high resolution and saturated colours on a large screen [1]. However, at present the main factor preventing a wide application the LCRT is the problem of its efficient operation without strong cooling, i.e., at temperatures close to room temperature. It was shown earlier [2 – 5] that at high radiation powers of the LCTR, the temperature of each point of the active region increases more than by 100 K during excitation by a tightly focused electron beam. As a result, the temperature of the entire active element increases upon quasi-continuous scanning because of the averaged heating. It is well known that the lasing threshold of semiconductor lasers (diode lasers and electron-pumped lasers) drastically increases with temperature, and their differential efficiency decreases in some cases. As a rule, the temperature dependence of the lasing threshold is described by an exponential with some characteristic temperature T_0.

The temperature regime of active elements was earlier studied in papers [3, 4] mainly upon cooling with liquid nitrogen. Since then considerable advances have been achieved in the room-temperature operation of the LCRT, mainly due to the improved technology of manufacturing laser screens (LSs). However, the optimal variant of raster scanning, which can provide the maximum average power of the LCRT in the continuous regime at room temperature, is still not established finally. In this paper, we study the temperature regime of the LS with the aim of optimising raster scanning.

V.I.Kozlovsky, Kh.Kh.Kumykov, I.V.Malyshev, Yu.M.Popov P.N.Lebedev Physics Institute, Russian Academy of Sciences, Leninsky prosp. 53, 119991 Moscow, Russia

Received 17 December 2001
Kvantovaya Elektronika **32** (4) 297 – 302 (2002)
Translated by M.N.Sapozhnikov

2. Formulation of the problem

The typical LS of a real LCRT is a sapphire disc of diameter 60 mm and thickness 6 mm, with a thin 15 μm thick semiconductor plate of diameter 50 mm cemented to it with an epoxy glue layer of thickness 5 μm. The plate has Al_2O_3 and TiO_2 mirror coatings of thickness no more than 1 μm deposited on both its sides and a ~ 0.1 μm Al layer deposited from the side of the incident electron beam. The sapphire disc is cooled with the water-alcohol mixture flow from the side opposite to the plate.

The exciting electron beam has a circular symmetry, and the current density in the electron-beam spot is usually described by the Gaussian distribution. The distribution of energy losses of the electron beam over the crystal depth is often described by a Gaussian shifted inside the crystal [6]. Upon raster scanning of interest to us, the electron beam sequentially runs through line after line, by filling the area of a rectangle by them. It is most important to determine the temperature of the active region at the instant of lasing, which virtually coincides with the instant of excitation by the electron beam. In this case, the time dependence of the distribution of temperature over the LS will be also found.

The direct numerical solution of the nonstationary heat conduction equation for a three-dimensional structure tending to a stationary regime involves time-consuming calculations. However, by using some properties of the excitation regime and the real parameters of the heat conduction of the structure layers, we can considerably simplify the problem. Because the thickness of the sapphire disc is much smaller than the raster size, the boundary conditions on the disc edges will not affect substantially the temperature distribution over a greater part of the raster area. For this reason, it is reasonable to use instead of the sapphire disc a sapphire substrate with a rectangular face corresponding to the raster shape. In his case, we will assume that heat is removed not through the side faces but only through the opposite side of the substrate cooled by the liquid flow. Fig. 1 shows the scheme of such a LS.

In this scheme, we also excluded mirror coatings from analysis. The upper mirror consists of more light atoms than in the semiconductor plate, so that, even having a thickness of 1 μm, it is sufficiently transparent for the 50-keV electron

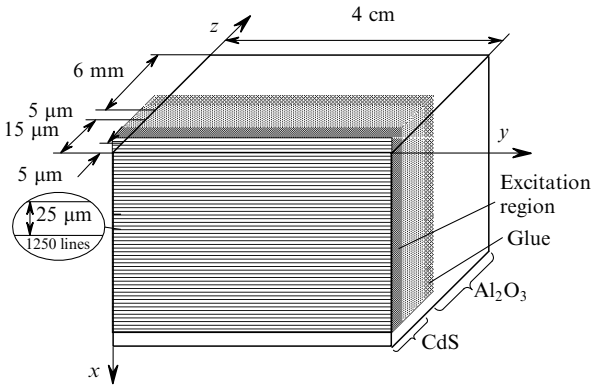

Figure 1. Scheme of the LS used for the calculation of the temperature profile.

beam, which we use in our calculations. On the other hand, the heat conduction of the lower mirror is greater than that of the glue layer, which is thicker in addition. Therefore, the influence of this mirror on the distribution of temperature in the semiconductor plate is far weaker that that of the glue layer and can be neglected. Further, we use for simplicity in our calculations the electron beam that produces a square spot on the LS with the homogeneous distribution of the current density over the spot. The side of the square spot is $d_e = 25$ μm. We also assume that the excitation energy $E_e = 50$ keV is distributed uniformly inside the crystal up to the depth $\delta = 5$ μm. This simplification is reasonable in analysis of the average heating and even heating caused by the adjacent lines, when the heat transfer over the distances greater than the characteristic size of the excitation inhomogeneity plays a key role.

The temperature of the active region affects the lasing regime of the LS only during excitation. It was found experimentally [7] that upon a single scan along a line ($E_e =$ 50 keV), for the electron beam current $I = 2$ mA and $d_e = 25$ μm, the maximum radiation power of LSs made of CdS (the lasing wavelength is 520 nm), CdSSe (620 nm), and ZnSSe (455 nm) at room temperature was achieved for scanning velocities $v_{sc} = (3-6) \times 10^5$ cm s^{-1}. For these parameters, the excitation time t_p of one pixel of diameter d_e is 8–16 ns. An adjacent pixel located at a distance of d_e in the direction of scan along the line is excited after the delay time of $0.5t_p$. The heat released in a previous pixel can propagate for 8 ns by a distance of the order of $r_p = [\lambda t_p/(\rho c_V)]^{0.5}$, where λ, ρ, and c_V are the heat conduction, density, and specific heat of the II–VI compound from which the semiconductor LS plate was made. For CdS (green emission LS), these quantities are 0.2 W K^{-1} cm^{-1}, 4.82 g cm^{-3}, and 0.3 J g^{-1} K^{-1}, respectively, and we obtain the estimate of $r_p = 0.4$ μm, which is considerably lower than d_e.

In contrast to this, an adjacent pixel located at a distance of d_e in the perpendicular direction, i.e., the nearest pixel on the next line (in the progressive scan regime without free intervals between the lines) will be excited after the time equal to the period of the line scan $t_l = l/v_{sc} + t_r \approx 13$ μs, where $l = 4$ cm is the line length and t_r is the reverse run duration. The heat from an adjacent pixel on the previous line will propagate during this time by the distance $r_l =$ 15 μm, which is comparable with d_e and, therefore, should be taken into account.

The above estimates show that the distribution of temperature in each cross section of the LS perpendicular to the scan along the line should be identical and differ only in the time delay corresponding to the movement of the electron beam along the line. In this case, the scan along the line can be replaced by the simultaneous pulsed excitation of the entire line during time t_p, assuming that the next line is also excited by the pulse after the time t_l. In this case, the electron-beam energy supplied to the entire line per pulse is $E_l = k_e IUl/v_{sc}$ and the specific supplied energy is $\varepsilon = k_e IU/(d_e v_{sc}\delta)$, where k_e is a coefficient determining the fraction of the energy of the incident electron beam entering inside the semiconductor and U is the accelerating voltage. All this will result in the adiabatic increase in the temperature by $\Delta T_p = \varepsilon/(c_V\rho)$.

Because the time t_p in our model is much shorter than the line period t_l, we will ignore the finiteness of the excitation time in calculations and will describe a thermal source by the delta function. Then, the heat conduction equation can be written in the form

$$c_V(z)\rho(z)\,\frac{\partial T}{\partial t} = \nabla[\lambda(z)\nabla T(x,z,t)] + f(x,z,t), \qquad (1)$$

where

$$f(x,z,t) = \sum_p \sum_n \varepsilon\{\theta[x-(n-1)d_e] - \theta(x-nd_e)\}$$

$$\times[\theta(z) - \theta(z-\delta)]\delta[t-(n-1+pN)t_l] \qquad (2)$$

is the power density of thermal sources in the scanning regime without a free interval between two lines (progressive scanning); θ is the Heaviside function; n is the number of scanned lines, which takes values from unity to N; p is the number of scanned frames; and N is the number of lines in the frame. The scheme of the LS and thickness of different layers are shown in Fig. 1, and the main thermal parameters of these layers are presented in Table 1. We will also assume below that the temperature of the opposite side of the sapphire substrate cooled, for example, by a liquid flow is known. Our estimates show that a real temperature drop between sapphire and liquid (away from sapphire) can be reduced down to several degrees by using an appropriately designed cooling system with a sufficient flow rate of the coolant.

Table 1. Heat conduction λ, specific heat c_V, and density ρ of different layers used in the calculation of the temperature regime of the LS [8, 9].

Active layer	λ/W cm^{-1} K^{-1}	c_V/J K^{-1} g^{-1}	ρ/g cm^{-3}
CdS	0.2	0.33	4.82
ZnSe	0.19	0.36	5.26
CdSe	0.09	0.26	5.81
ZnS	0.27	0.47	4.09
YAG	0.13	–	4
Sapphire	0.4	0.8	3.97
Glue	0.005	0.4	1.2

The numerical solution of Eqn (1) with the thermal source (2) within the first frame becomes stationary quite rapidly. The stationary regime is caused by the influence of the previous heated lines. It is obvious that this influence can be reduced by increasing the distance between the adjacent

lines. To analyse this effect in the usual scanning regime, when the first half-frame is scanned by a half number of the lines, with the interval between the lines equal to the line length, while the second half-frame is scanned by the lines that are located between the lines of the first half-frame (interlaced scanning), the thermal source function should be written in the form

$$f(x,z,t) = \sum_p \Big\{ \sum_{n=2k+1} \varepsilon\{\theta[x-(n-1)d_e] - \theta(x-nd_e)\} \times [\theta(z)-\theta(z-\delta)]\delta[t-(n-1+2pN)t_l/2] + \sum_{n=2k+2} \varepsilon\{\theta[x-(n-1)d_e] - \theta(x-nd_e)\} \times [\theta(z)-\theta(z-\delta)]\delta\{t-[n-2+(2p+1)N]t_l/2\}\Big\}, \quad (3)$$

where k is an integer between zero and $N/2-1$.

During the time of frame scanning (1/60 s), the heat from the first lines will propagate by the distance of the order of $r_f = 0.44$ mm (r_f was estimated similarly to r_p and r_l), and the distribution of temperature behind these lines can be assumed homogeneous because of the diffusion miing at any cross section perpendicular to the z axis. When this heat will reach the cooled sapphire surface (for a few seconds in our case), a quasi-stationary regime will be established. By solving Eqn (1) with a source independent of x

$$f(z,t) = \sum_p \varepsilon[\theta(z)-\theta(z-\delta)]\delta(t-pNt_l), \quad (4)$$

we can determine the mean temperature ΔT_{av} of the active region before excitation by the electron beam and before coming of the heat from the previous line, as well as the temperature profile of the LS for $z > r_f$ determined by the cooling of the entire LS.

We distinguished above three thermal processes: almost adiabatic heating during the commutation of one LS pixel by the electron beam, the heating caused by the thermal flow from previous lines, and the averaged heating –a pedestal determined by the LS cooling as whole. Each of these processes leads to the increase in the temperature of the active region by ΔT_p, ΔT_l, and ΔT_{av}, respectively. One should bear in mind that the temperature rise ΔT_{av} near the surface differs from the temperature rise

$$\Delta T_{st} = \Delta T_s + \Delta T_g + \Delta T_{sub}, \quad (5)$$

which is obtained by solving the one-dimensional stationary heat conduction problem with the equivalent thermal flow

$$P_{eff} = \frac{k_e IU}{d_e v_{sc} N t_l} = \frac{\lambda_s \Delta T_s}{h_s} = \frac{\lambda_g \Delta T_g}{h_g} = \frac{\lambda_{sub}\Delta T_{sub}}{h_{sub}},$$

where ΔT_s, ΔT_g, ΔT_{sub}, h_s, h_g, h_{sub} and λ_s, λ_g, λ_{sub} are the temperature drops in the semiconductor layer, glue layer, substrate (sapphire), their thickness, and heat conduction, respectively. For $z < r_f$, at the instant of time before the next excitation pulse, we have $\Delta T_{av} < \Delta T_{st}$, because the heat moves away from the surface by the distance r_f. For this reason, ΔT_{av} will strongly depend on the period of frame scanning near the LS surface. For $z > r_f$, the temperature gradient produced inside sapphire in the stationary regime should be almost the same for stationary and non-stationary processes.

3. Results of numerical calculations

Fig. 2a shows the distribution of temperature near the CdS LS surface (in a layer of thickness δ) along the direction of frame scanning (the x axis) at the instants of time directly after the next excitation pulse. The distribution was calculated by numerically solving Eqn (1) with the source (2), in which $p = 0$ (excitation during the first frame is considered) and the first twenty terms of the sum over n are absent (the electron beam is switched on only after the 21st line.) The latter condition was chosen in order to exclude the influence of the edge boundary on the temperature distribution). We used the following parameters in calculations: $d_e = 25$ μm, $\delta = 5$ μm, $v_{sc} = 4.18 \times 10^5$ cm s^{-1}, $I = 2$ mA, $U = 50$ kV, $t_l = 13.3$ μs, $l = 4$ cm, and $k_e = 0.75$. In this case, the pulsed adiabatic increase in the temperature of the line was $\Delta T = 90.4$ K.

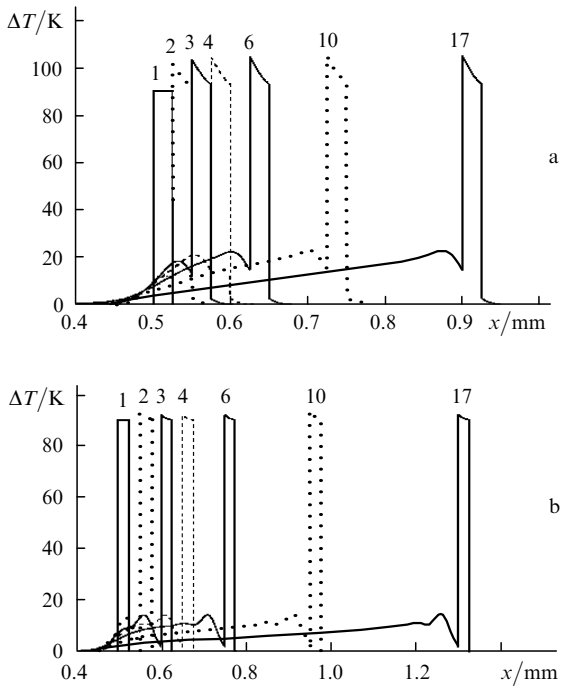

Figure 2. Distributions of the heating $\Delta T = \Delta T_l + \Delta T_p$ of the CdS LS active layer along the x axis at the instants of time directly after the 1, 2, 3, 4, 6, 10, and 17th line excitation pulses obtained by numerically solving Eqn (1) (a) with the source (2), in which $p = 0$ (excitation during the first frame is considered) and the first 20 terms of the sum over n are absent (the electron beam is switched on beginning from the 21st line) and (b) with the source (3), in which the electron beam is switched on beginning from the 11st line of the first frame for $d_e = 25$ μm, $\delta = 5$ μm, $L_c = 15$ μm, $v_{sc} = 4.18 \times 10^5$ cm s^{-1}, $I = 2$ mA, $U = 50$ kV, $t_l = 13.3$ μs, $l = 4$ cm, $k_e = 0.75$, the glue layer thickness of 5 μm, and the sapphire substrate thickness of 6 mm.

One can see from Fig. 2a that the distribution of temperature over the excitation spot after the successive line pulse is stabilised already after the first five switched lines. Due to the heating caused by previous lines, the temperature varied over the spot from 3 to 15 K for the average $\Delta T_l = 9$ K. The heating ΔT_l will increase proportionally to the current and inversely proportionally to the electron-

beam scan velocity. To decrease this temperature increase, it is necessary to increase the distance between two successively scanned lines. Fig. 2b shows the results of similar calculations performed for interlaced scanning using the thermal source (3). In this case, the average temperature increase is negligible: $\Delta T_l = 1$ K. Thus, to exclude heating caused by previous lines, it is sufficient to use interlaced scanning.

Fig. 3 shows the results of the solution of Eqn (1) with the thermal source (4) before the next pulse for the same parameters of the calculation. One can see that the stationary regime is achieved approximately after 4 s, and the temperature increase near the LS surface in the stationary regime is $\Delta T_{av} \simeq 5.8$ K. This time can be decreased by a factor of four by decreasing the sapphire disc thickness by half. In this case, the value of ΔT_{av} will also decrease by half. The dotted curve shows the distribution of temperature inside the LS obtained by solving the one-dimensional stationary heat conduction equation. In this case, the temperature increase near the surface is related to a constant gradient and poor heat conduction of the glue layer. As mentioned above, the solutions of the stationary equation and Eqn (1) with the thermal source (4) differ from each other near the LS surface over the thickness approximately equal to r_f.

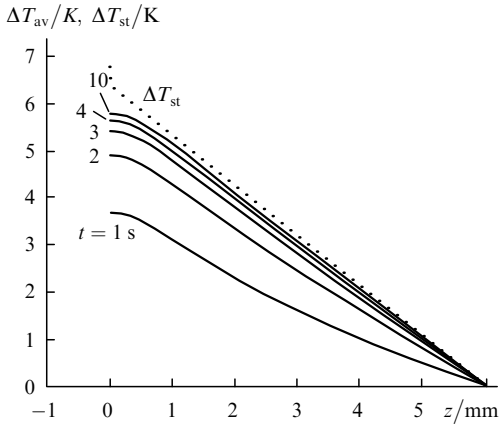

Figure 3. Distributions of the heating ΔT_{av} of the CdS LS surface along the z axis at the instants of time corresponding approximately to 1, 2, 3, 4, and 10 s after the beginning of the LS operation directly before the next excitation pulse obtained by numerically solving Eqn (1) with the thermal source (4) (the rest of the parameters are the same as in Fig. 2), as well as the solution ΔT_{st} (5) of the one-dimensional stationary heat conduction equation.

4. Effect of the temperature of the active region on lasing parameters

Consider the effect of the temperature of the active region on the lasing power. The lasing power can be written in the form

$$P = \eta(T) P_{in} \left[1 - \frac{j_{th}(T)}{j_{in}} \right], \tag{6}$$

where P_{in} and j_{in} are the pump power and the electron-beam current density; j_{th} is the threshold current density; $\eta = \eta_0 k_e k_l f_{h\nu}$ is the differential efficiency of conversion of the pump radiation to laser radiation; $\eta_0 \approx 0.35$ is the theoretical limit of the lasing efficiency upon electron-beam pumping [10]; $k_e \approx 0.75$ [11]; k_1 is a coefficient taking into account the transverse inhomogeneity of excitation, which is caused by the distribution of the current density in the electron-beam spot; and $f_{h\nu}$ is the output function of the laser emission. The temperature dependence of the threshold current for a typical CdS LS obtained upon single line scanning is presented in Fig. 4a.

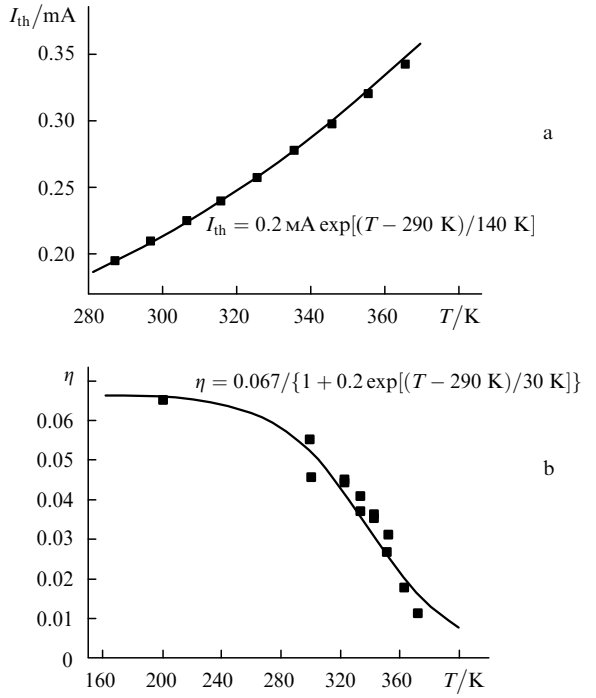

Figure 4. Temperature dependences of the threshold current I_{th} (a) and the differential lasing efficiency (b) for the CdS LS of thickness $L_c = 15$ μm for $U = 50$ kV, $d_e = 25$ μm and a single line scanning with $v_{sc} = 4 \times 10^5$ cm s^{-1}.

Because electron-beam excitation is strongly inhomogeneous, it is more convenient to measure a total current rather than the current density. We assume below that the diameter of the electron-beam spot on the LS does not depend on the current. By using the common exponential approximation of the temperature dependence of the threshold current

$$I_{th}(T) = I_r \exp\left(\frac{T - T_r}{T_0} \right), \tag{7}$$

we obtain the following best fit parameters for the experimental data shown in Fig. 4a: $T_r = 290$ K, $I_r(T_r) = 0.2$ mA, and $T_0 = 140$ K. One can see from Fig. 4b that the differential lasing efficiency decreases with increasing temperature. The temperature dependence of η is mainly determined by the temperature dependence of the output function $f_{h\nu}$, which in turn is determined by an increase in the intracavity losses with temperature. The efficiency $\eta(T)$ can be approximated by the function

$$\eta(T) = \frac{\eta_r}{1 + 0.2\exp[(T - T_r)/T_{01}]} \tag{8}$$

with parameters $T_r = 290$ K, $T_{01} = 30$ K, and $\eta_r = 0.067$.

Under real conditions, the temperature profile of the active region is strongly nonuniform [2, 3]. Pulsed heating produces a temperature gradient in the excitation region along the direction of line scanning at a depth of about 5 μm. Heating caused by the previous lines produces an additional gradient perpendicular to the line. Only the average heating produces the uniform increase in the temperature of the semiconductor plate.

An exact analysis of the effect of a temperature gradient is a complicated problem. Here, we will estimate the dependence of the lasing power on the electron-beam current only qualitatively using the following assumptions. We assume that the dependence of the differential lasing efficiency on the current is determined by the average heating of the semiconductor plate (average heating causes losses in the passive region of a cavity), while the effective threshold current depends on the temperature of the active region, which is determined by the average and adiabatic heating. We will neglect heating produced by adjacent lines because we can eliminate it by using interlaced scanning.

Then, we divide the excitation spot perpendicular to the direction of the temperature gradient into elementary strips of width dy with the temperature $T(y)$, whose output power can be determined from Eqn (6) taking into account expressions (7) and (8). The total output power is obtained by summation over all the strips. As a result, we obtain

$$P_{out} = U \frac{\eta_r}{1 + 0.2\exp(\alpha I/T_{01})} \times \int_0^{y_0} \left\{ I - I_r \exp\left[\frac{(\alpha + \beta y) I}{T_0} \right] \right\} \mathrm{d}y \,, \qquad (9)$$

where α and β are the proportionality coefficients between the current I and the average heating ΔT_{av} and between the current I and the maximum adiabatic heating ΔT_p; y_0 is the coordinate at which the integrand vanishes; $y_0 = 1$ if the integrand is positive for the given I and variation of y in the interval between 0 and 1.

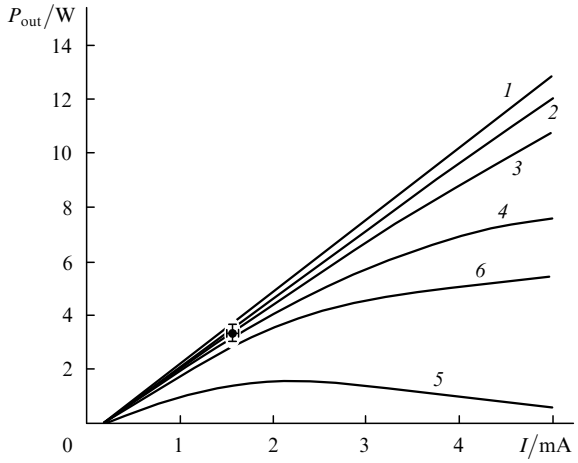

Figure 5. Light–current characteristics of the LS calculated for $T_0 = 140$ K, $I_r = 0.2$ mA, $T_{01} = 30$ K, and $\eta_r = 0.067$ neglecting the semiconductor heating by the electron beam (*1*), taking only the adiabatic heating into account for $\beta = 45.2$ (*2*), and taking the adiabatic and average heating into account for $\beta = 45.2$ (*3–5*) and 135 (*6*), $\alpha = 2.9$ (*3*), 8.7 (*4*), 25 (*5*), and 2.9 (*6*). The circle is the experimental result.

The results of calculations performed by expression (9) for different values of parameters α and β are presented in Fig. 5. One can see that the real case calculated in section 3 for the CdS LS and a 6 mm thick sapphire substrate for interlaced scanning with $v_{sc} = 4.18 \times 10^5$ cm s^{-1} ($\beta = 45.2$, $\alpha = 2.9$) only slightly differs from the case of pulsed excitation ($\beta = 45.2$, $\alpha = 0$) and the case when heating is neglected at all ($\beta = \alpha = 0$). However, the replacement of a sapphire substrate by a garnet substrate with a lower heat conduction ($\beta = 45.2$, $\alpha = 8.7$) results in a noticeable deterioration of the light–current characteristic. This characteristic further degrades when the line scanning frequency or the scanning velocity is decreased by three times ($\beta = 135$, $\alpha = 2.9$) and also when the sapphire substrate is insufficiently cooled by water ($\beta = 45.2$, $\alpha = 25$). One can also see from Fig. 5 that, when the scanning parameters, the cooling system, and the thickness of LS layers are chosen properly, the increase in the output power up to 10 W is not limited by temperature effects.

5. Conclusions

The study of the temperature regime of the active element of the LCRT operating in the raster scanning regime has revealed three basic factors determining temperature in the active medium during its excitation: pulsed adiabatic heating of a pixel during excitation by the electron beam, heating produced by adjacent lines, and average heating determined by cooling of the LS. The estimate of the temperature increase caused by these factors at room temperature for the real parameters of the electron beam showed that pulsed heating can be reduced by increasing the scanning velocity. The heating caused by the lines scanned previously can be reduced by using interlaced scanning, while the average heating can be reduced by decreasing the thickness of a heat-conducting substrate. The heating of the active region limits an increase in the output power with increasing the electron-beam current. Our estimates have shown that the heating of the active region does not prevent increasing the current up to 5 mA and the power density up to 10 W for active elements made using the technology available at present. However, other limitations are possible, which can be related, for example, to the degradation of glue layer or mirror coatings, which calls for further investigations.

Acknowledgements. This work was supported by the Russian Foundation for Basic Research (Grant No. 01-02-16409) and the 'Leading Scientific Schools' program (Grant No. 00-15-96624).

References

1. Nasibov A.S., Kozlovsky V.I., Reznikov P.V., Skasyrsky Ya.K., Popov Yu.M. *J. Cryst. Growth*, **117**, 1040 (1992).
2. Kozlovsky V.I., Nasibov A.S., Pechenov A.N., Reznikov P.V., Skasyrsky Ya.K. *Kvantovaya Elektron.*, **5**, 487 (1978) [*Sov. J. Quantum Electron.*, **8**, 281 (1978)].
3. Kozlovsky V.I., Nasibov A.S., Pechenov A.N. *Preprint FIAN* (24) (Moscow, 1978).
4. Ulasyuk V.N. *Kvantoskopy* (Quantoscopes) (Moscow: 'Radio i Svyaz', 1988).
5. Eliseev P.G., Popov Yu.M. *Kvantovaya Elektron.*, **24** 1067 (1997) [*Quantum Electron.*, **27**, 1035 (1997)].

6. Bogdankevich O.V., Darznek S.A., Eliseev P.G. *Poluprovodnikovye lazery* (Semiconductor Lasers) (Moscow: Nauka, 1976).
7. Kozlovsky V.I., Nasibov A.S., Reznikov P.V. *Kvantovaya Elektron*., **8**, 2493 (1981) [*Sov. J. Quantum Electron*., **11**, 1522 (1981)].
8. Hartmann H., Mach R., Selle B., in *Wide Gap II–VI Compounds as Electronic Materials. Current Topics in Materials Science* (Amsterdam: North-Holland, 1982) Vol. 9, p. 1.
9. Grigor'ev I.S., Meilikhov E.Z. (Eds) *Fizicheskie velichiny. Spravochnik* (Handbook of Physical Quantities) (Moscow: Energoatomizdat, 1991).
10. Popov Yu.M. *Trudy FIAN*, **31**, 3 (1965).
11. Klein C.A. *IEEE J. Quantum Electron*., **4**, 186 (1968).